ARTICLE

Exploring the Chemical Sensitivity of a Carbon Nanotube/Green Tea Composite

Yanan Chen,[†] Yang Doo Lee,[†,‡] Harindra Vedala, Brett L. Allen, and Alexander Star*

Department of Chemistry, University of Pittsburgh and the National Energy Technology Laboratory, Pittsburgh, Pennsylvania 15260, United States. [†]These authors contributed equally to this work. [‡]Present address: Display and Nanosystem Laboratory, College of Engineering, Korea University, Seoul, Republic of Korea.

ABSTRACT Single-walled carbon nanotubes (SWNTs) possess unique electronic and physical properties, which make them very attractive for a wide range of applications. In particular, SWNTs and their composites have shown a great potential for chemical and biological sensing. Green tea, or more specifically its main antioxidant component, epigallocatechin gallate (EGCG), has been found to disperse SWNTs in water. However, the chemical sensitivity of this SWNT/green tea (SWNT/EGCG) composite remained unexplored. With EGCG present, this SWNT composite should have strong antioxidant properties and thus respond to reactive oxygen species (ROS). Here we report on fabrication and characterization of SWNT/EGCG thin films and the measurement of their relative conductance as a function of H_2O_2 concentrations. We further investigated the sensing mechanism by Fourier transform infrared (FTIR) spectroscopy and field-effect transistor measurements (FET). We propose here that the response to H_2O_2 arises from the oxidation of EGCG in the composite. These findings suggest that SWNT/green tea composite has a great potential for developing simple resistivity-based sensors.

KEYWORDS: resistivity sensors · ROS · hydrogen peroxide · relative humidity

Single-walled carbon nanotubes (SWNTs) continue to be of increasing importance in a variety of areas including materials and life sciences.[1−8] Because of their size (approximately 1−3 nm in diameter, 1 μm long) and their unique physical and electronic properties, that is to say, high tensile strength, chemical stability, and electrical conductivity, SWNTs are an ideal material to interface with biological systems. For many biological applications, however, their dispersibility in aqueous media becomes the main problem. There have been a variety of methods developed to increase dispersion of this material in water by noncovalent functionalization including using surfactants,[9] polymers,[10,11] and biomolecules such as DNA, peptides, polysaccharides, and proteins.[12−15] Recently, it has been shown that green tea can disperse nanotubes in aqueous solutions.[16]

Made solely from the leaves of *Camellia sinensis*, green tea has undergone extensive research for its antioxidant abilities.[17] Specifically, antioxidant properties can be derived from the presence of catechins. These organic compounds, which are a group of water-soluble polyphenols,[18] consist of epicatechin (EC), epicatechin gallate (ECG), epigallocatechin (EGC), and epigallocatechin gallate (EGCG).[19] Studies have shown that such compounds possess biological activity exhibiting not only antioxidant behavior[20,21] but antitumor[22,23] and anticancer[24−26] effects as well. Among antioxidants present, EGCG is the most abundant and has the strongest activity.[27] This compound reacts readily with reactive oxygen species (ROS) such as superoxide (O_2^-), hydroxyl radicals (•OH), and hydrogen peroxide (H_2O_2).[28]

Here we examine the chemical sensitivity of a SWNT/EGCG composite to H_2O_2 exposure. This composite material was characterized by transmission electron microscopy (TEM), atomic force microscopy (AFM), Fourier transform infrared (FTIR) spectroscopy, Raman spectroscopy, and ultraviolet−visible−near-infrared (UV−vis−NIR) absorption spectroscopy in thin films. Additionally, electrical conductivity of the SWNT/EGCG composite was measured on interdigitated Au electrodes upon exposure to H_2O_2 vapors, relative humidity, and varying concentrations of H_2O_2 in water. Two different device architectures, namely, a SWNT/EGCG premixed composite and a SWNT/EGCG layer-by-layer composite, were tested for their response to H_2O_2. The mechanism of the electrical response to H_2O_2 was further evaluated by comparing the SWNT/EGCG composite with bare SWNTs and by adding Fe_2O_3 nanoparticles (NPs) into the composite in order to generate •OH radicals by Fenton catalysis.[29] We also performed FTIR spectroscopy and studied the response of a SWNT/green tea

*Address correspondence to astar@pitt.edu.

Received for review November 3, 2009 and accepted October 25, 2010.

Published online November 2, 2010.
10.1021/nn100988t

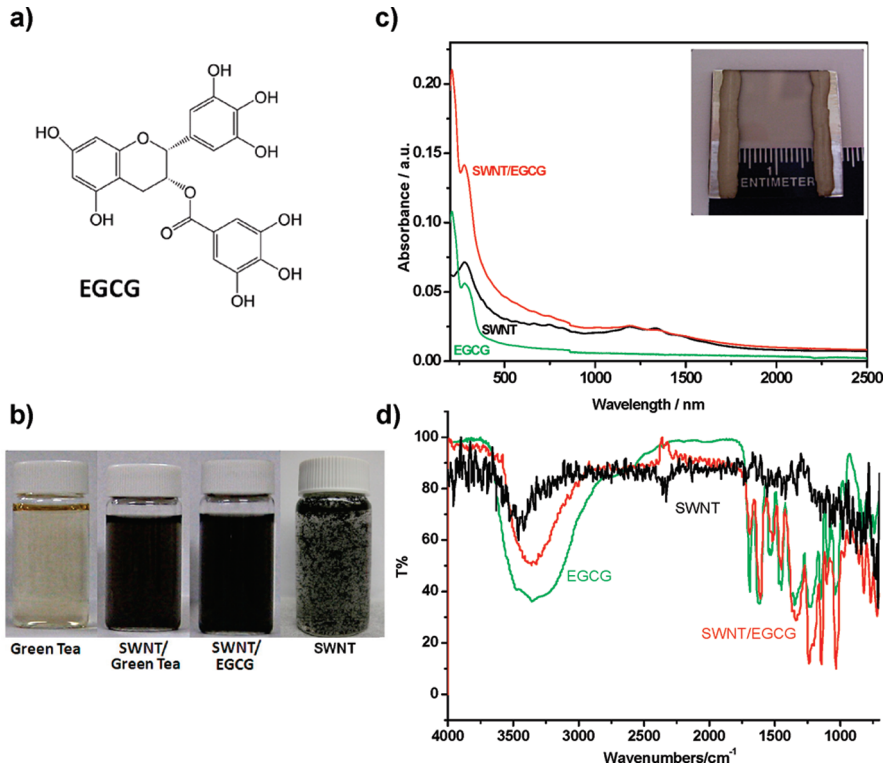

Figure 1. (a) Chemical structure of epigallocatechin gallate (EGCG). (b) Photograph of four vials with green tea (left), SWNT and green tea (middle left), 4.4 × 10^{-4} M EGCG sonicated with *ca.* 1 mg of SWNTs (middle right) and SWNTs in water (right). (c) UV−vis−NIR absorption spectra of SWNT (black), EGCG (green), and SWNT/EGCG (red) as thin films on quartz. Inset displays a photograph of transparent SWNT/EGCG conductive film on a quartz slide. (d) FTIR spectrum of bare SWNTs (black), EGCG in MeOH (4 × 10^{-4} M) (green), and SWNT/EGCG composite after heating at 140 °C for 20 min (red).

composite in a three-electrode electrolyte-gated field-effect transistor (FET) configuration to investigate the sensing mechanism.

RESULTS AND DISCUSSION

Using green tea and EGCG (Figure 1a), SWNTs were dispersed in water through sonication. Figure 1b shows these suspensions in water, which were stable for up to three months. As the catechin comprises phenol groups, it is thought that dispersion occurs through $\pi-\pi$ stacking with the nanotube's graphitic lattice. Presumably, the noncovalent interaction between SWNTs and cathechin leads to the disaggregation of SWNT bundles and provides a stable dispersion by sonication.[16] To study the interaction between EGCG and carbon nanotubes, spectroscopic measurements were taken of a spray-cast film on a quartz slide using UV−vis−NIR spectroscopy. The resulting spectrum is a superposition of SWNTs and EGCG spectra (Figure 1c), in a good agreement with previous solution studies.[16] It should be mentioned here that the thin films of the SWNT/EGCG composite for UV−vis−NIR studies were prepared by spray-casting the solution to a quartz slide at 140 °C to prevent nanotube agglomeration through drying and provide uniform films. EGCG was stable to this thermal treatment because, after the heating, the EGCG absorption spectrum in the composite demonstrates no shift compared to pure EGCG (prepared by drop-casting EGCG solution and drying at room temperature) (Figure 1c). Furthermore, an FTIR spectrum of the SWNT/EGCG composite (heated at 140 °C for 20 min) showed peaks (*e.g.*, 3360, 1610, 1450, and 1140 cm^{-1}) characteristic of EGCG (in MeOH), yet additional evidence of the composite thermal stability (Figure 1d). In fact, the SWNT/EGCG composite shows no degradation up to 200 °C, according to thermogravimetric analysis (TGA) (Figure S1, Supporting Information). Combined with TGA results, the spectroscopic results confirm that this composite is stable at the temperature we adopted to prepare the thin films. Interactions between SWNTs and EGCG in the composite were further characterized by Raman spectroscopy. The Raman spectra of a SWNT/EGCG composite and pristine SWNT were mostly similar (Figure S2), indicating noncovalent interaction between EGCG and SWNT with a negligible effect on SWNT vibration modes.[30] To confirm EGCG coverage and provide information about composite surface morphology, we characterized the composite using AFM and TEM. In AFM images, the surface of the SWNT/EGCG composite appears to be covered unevenly (Figure S3a), clearly showing different morphology from pristine SWNTs (Figure S3b). Similar change in morphology was observed in TEM imaging. SWNTs in the composite are covered with an amorphous coating (Figure S4). Because of the difficulty in dispersing pristine SWNTs in water (refer to Figure 1b), for AFM and

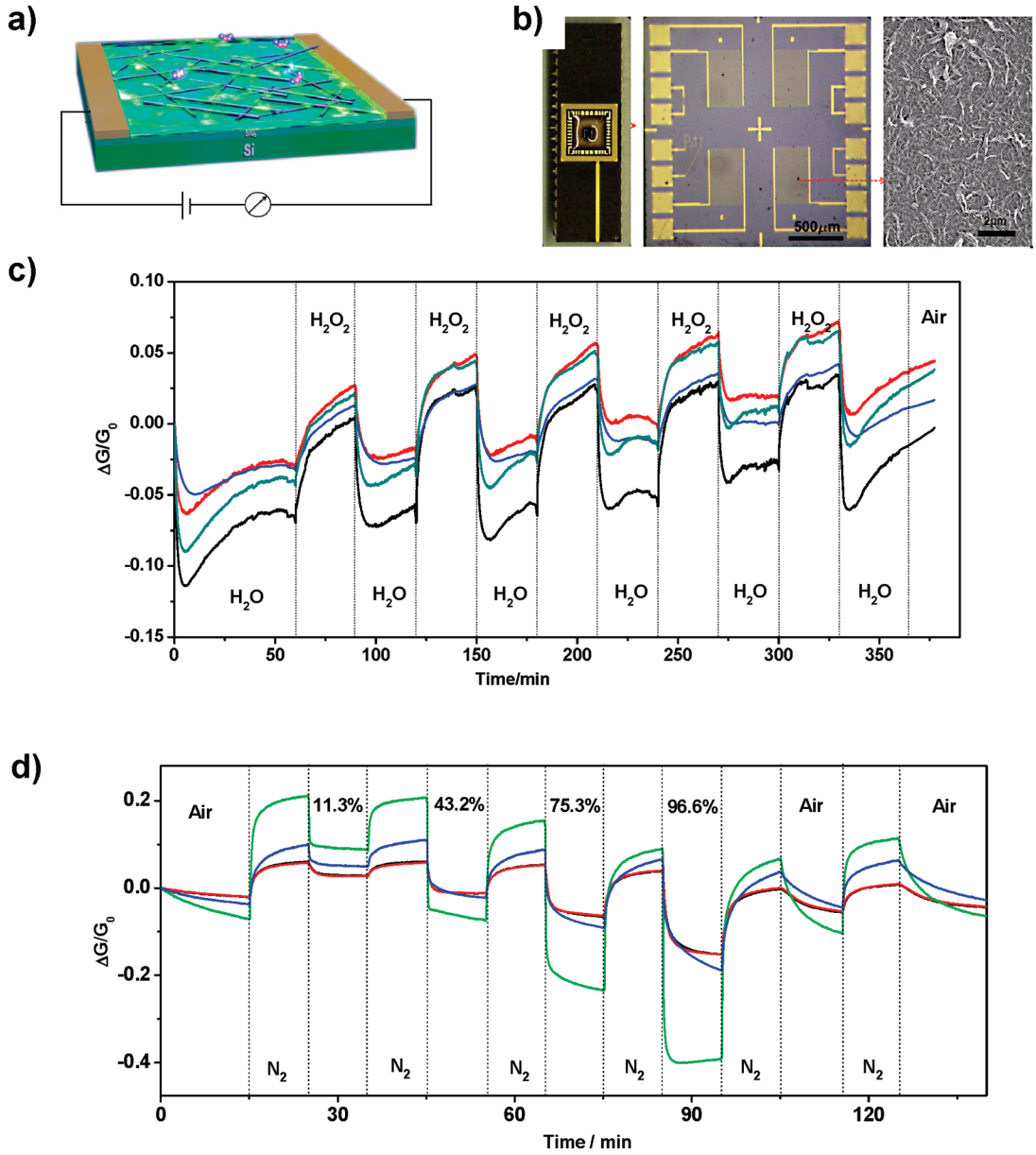

Figure 2. (a) Schematic illustration of a SWNT/EGCG composite device consisting of Si/SiO_2 substrate and metal contacts. (b) Optical images (scale bar = 500 μm) and scanning electron microscope (SEM) image (scale bar = 2 μm) of the SWNT/EGCG film deposited on CERDIP package with a Si chip containing four interdigitated Au electrodes (interelectrode spacing of 10 μm). (c) Relative conductance *versus* time dependence of four interdigitated devices (shown in different colors) coated with the SWNT/EGCG composite cycled between H_2O_2 and H_2O vapor pulses (H_2O_2 concentration was calculated as 45 ppm). (d) Relative conductance *versus* time dependence of four interdigitated devices coated with the SWNT/EGCG composite cycled between dry N_2 and N_2 bubbled through different saturated salt solutions generating different levels of relative humidity (%).

TEM, we used SWNT suspension in DMF to provide information of uncovered, bare SWNTs.

The thin films of the SWNT/EGCG composite were both transparent and conductive (Figure 1c, inset). The electrical conductance of the films (10 films) was measured as 271 ± 61 μS. These values are comparable to 325 ± 105 μS conductance of thin films made from bare SWNTs (13 films) prepared by spray coating a SWNT suspension in DMF at 180 °C. Taken into account the thin film thickness measured by AFM (Figure S5a), the conductivities can be calculated as 22.9 ± 5.1 and 27.4 ± 8.9 S/cm for SWNT/EGCG and SWNT thin films, respectively (see Supporting Information for calculation details). The small decrease in the thin film conductivities could be due to the conformal coating of EGCG on the individual SWNTs, thereby causing an increase in internanotube separation.

In order to examine the chemical sensitivity of the composite to varying concentrations of H_2O_2, vapors SWNT/EGCG composite devices were fabricated by drop-casting SWNT/EGCG on Si chips with four interdigitated Au electrodes (Figure 2). Conductance measurements on composite devices were carried out on a custom test-board using Zephyr software.[31] Using a

Keithley 2602 dual-source meter and Keithley 708A switching mainframe, we monitored all devices on a single chip at a given time.

We first investigated the effect of H_2O_2 vapors by measuring relative conductance ($\Delta G/G_0$) *versus* time as H_2O_2 vapors were pulsed using N_2 as a carrier gas. Devices were tested under a constant applied voltage of 50 mV at room temperature. H_2O_2 vapors were pulsed at 30 min intervals, with saturated water vapor acting as the "off" state. Water and H_2O_2 vapors were generated by passing 660 sccm (standard cubic centimeters per minute) of N_2 gas through bubblers filled with deionized water and 1 M H_2O_2 solution, respectively. As shown in Figure 2c, device exposure to H_2O_2 vapors resulted in a conductance increase and the device response was constant during the test. Bare SWNT devices, however, showed no obvious response to H_2O_2 vapors, and no stable baseline was achieved under device exposure to high relative humidity (Figure S6a). By using saturated water vapor as the "off" state, we attempted to isolate the composite response to H_2O_2 vapors from any effects of relative humidity. However, the effect was not fully eliminated. The H_2O_2 concentration in the vapor was calculated[32] to be 45 ppm, and its effect on the composite conductance was largely masked by the change in relative humidity. The measured relative humidities of H_2O vapor and H_2O_2 vapor were 92 and 80%, respectively.

In fact, SWNT/EGCG composite devices have a large response to water vapors. Figure 2d shows the normalized response of the composite device to the effects of relative humidity by pulsing varying relative humidity using N_2 as a carrier gas. Briefly, controlled relative humidity was created by passing N_2 gas through different saturated salt solutions including LiCl, K_2CO_3, NaCl, and KH_2PO_4 corresponding to relative humidities of 11.3, 43.2, 75.3, and 96.6%, respectively.[33,34] Relative humidities were pulsed at 10 min intervals, with dry N_2 acting as the "off" state. As relative humidity increases, conductance of SWNT/EGCG devices decreases. It is also quite notable that this response is 1 order of magnitude larger for the SWNT/EGCG composite over that of bare nanotubes (Figure S6b,c).

Such a decrease in conductance for the SWNT/EGCG composite is typical of most SWNT/polymer composites.[35,36] EGCG, hydrophilic in nature, has a high affinity for water. As this layer gets hydrated, two effects may occur. The first effect involves the expansion of the EGCG composite, at high relative humidity, as we confirmed by volume change of the composite. The composite expands twice when relative humidity is increased from 0 to 100% (Figure S7). As swelling of this composite occurs, nanotubes are separated further apart and the percolation through the SWNT network is decreased, resulting in a decrease in conductance. Additionally, water molecules can create charge traps on nanotube networks,[37] resulting in the change in the conductance.

To overcome effects of relative humidity, we performed liquid measurements. The stability of the SWNT/EGCG thin films in aqueous environment was tested by measuring the thickness of the thin films before and after their exposure to water for 4 h and monitoring the conductance of the thin film immersed in water. The small variation in the thin film thickness (Figure S5a,b) and the stable conductance over the test time (Figure S5c,d) indicated insignificant leaching and confirmed the film stability. We have already made mention that EGCG is a strong antioxidant and, as such, should have a specific response for ROS such as H_2O_2, as opposed to response of the thin films to water. In liquid measurements, the composite should be fully hydrated, and thus, the conductance change will be only due to the result of ROS in the solution. We examined SWNT/EGCG composite devices for changes in conductance in real time. Devices were initially exposed to four additions of 10 μL of deionized water to create a stable hydrated layer within SWNT/EGCG composites. As can be seen from Figure 3a, the initial exposure to 10 μL of water elicited the same conductance decrease as witnessed in the relative humidity experiments. After four additions of deionized water, any subsequent response should be solely due to the concentrations of H_2O_2. An addition of 10^{-4} M H_2O_2 (10 μL) resulted in a slight increase in the conductance of the device. Then the higher concentrations of H_2O_2 (10^{-3} and 10^{-2} M) were added subsequently, and the responses increased accordingly. As a control experiment, bare nanotube devices were tested for the same concentrations of H_2O_2, as well as the initial additions of deionized water. As can be seen from Figure 3b, after additions of deionized water, the bare SWNT device cannot reach a stable baseline as effectively as the SWNT/EGCG composite, which may be due to the hydrophobicity of bare nanotubes, and the device has no obvious response to the subsequent additions of H_2O_2.

The response of the SWNT/EGCG composite to H_2O_2, however, is relatively smaller than the response to water. To explore a method to improve the H_2O_2 response, we adopted layer-by-layer architecture to fabricate the SWNT/EGCG device (Figure 3c, inset). We first deposited SWNTs (DMF suspension) onto the electrodes using a dielectrophoresis (DEP) method.[38] After washing with DMF and drying at 180 °C, the chips were incubated with EGCG solution (in water, 4.4×10^{-4} M) for 2 h to deposit EGCG on the surface of SWNTs and then washed with deionized water and dried in ambient conditions. This device architecture demonstrated improved response to H_2O_2 (Figure 3c). H_2O_2 concentration as low as 5×10^{-6} M was detected with signal-to-noise ratio of 8. The improvement in the sensor performance can be attributed to two factors, namely, dielectrophoretic assembly of nanotube between the

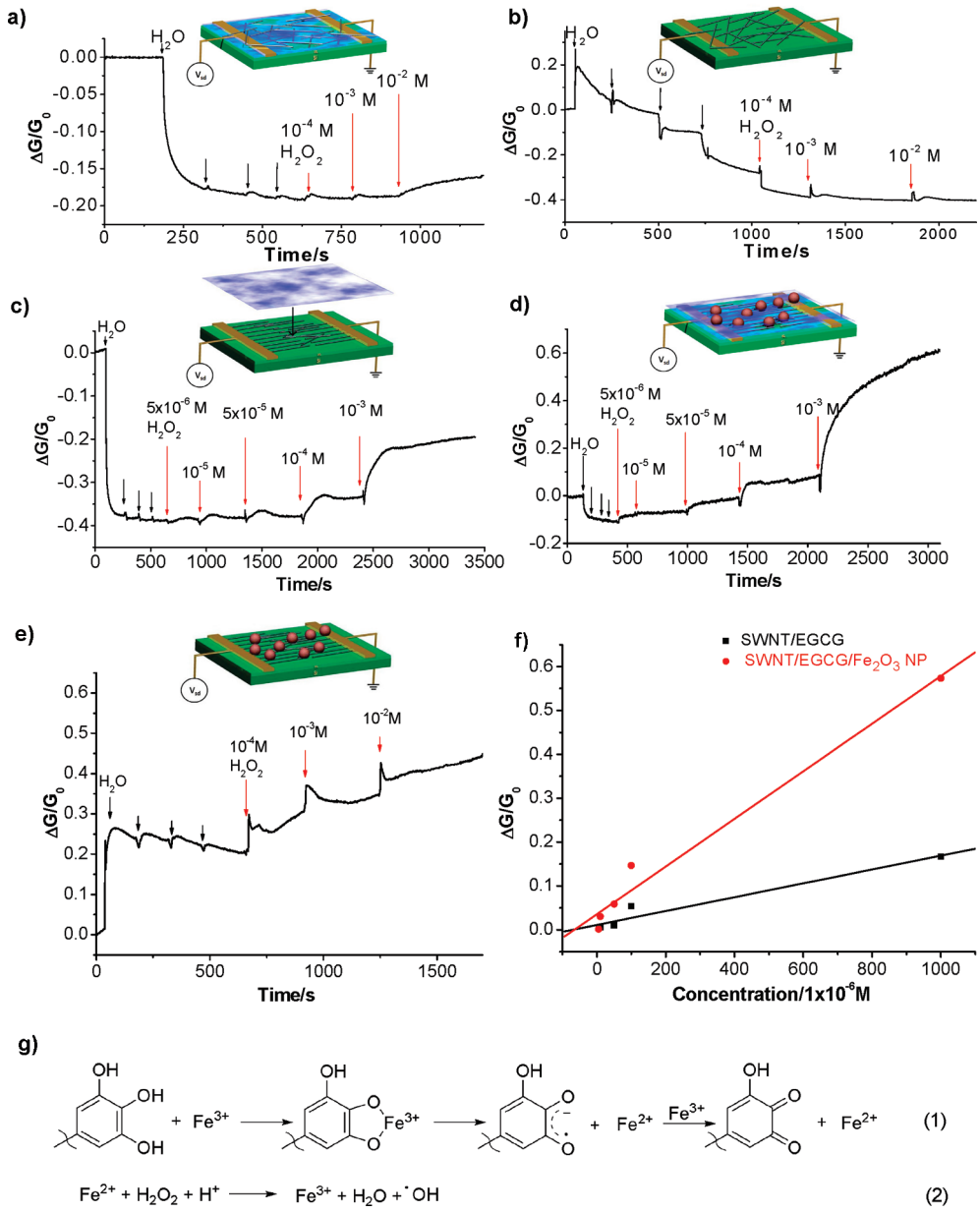

Figure 3. Relative conductance *versus* time response to varying concentrations of H_2O_2 of (a) SWNT/EGCG premixed composite, (b) bare SWNT device, (c) SWNT/EGCG layer-by-layer composite, (d) SWNT/EGCG/(Fe_2O_3 nanoparticles) layer-by-layer composite, and (e) SWNT/(Fe_2O_3 nanoparticles) layer-by-layer composite. Insets show the schematic device architectures. (f) Relative conductance change *versus* concentration plot of SWNT/EGCG (black) and SWNT/EGCG/(Fe_2O_3 nanoparticles) (red). (g) Fenton's catalysis mechanism includes the coordination of Fe^{3+} by polyphenols in EGCG, subsequent iron reduction and semiquinone formation, and reduction of Fe^{3+} to form a quinone species and Fe^{2+} (reaction 1). H_2O_2 is reduced by Fe^{2+}, resulting in the formation of ●OH radical (reaction 2).[43]

metal electrodes and layer-by-layer deposition of EGCG on bare SWNTs. DEP aids in alignment of the nanotubes between the electrodes and results in increased field-effect mobility as compared to devices fabricated by drop-casting.[39] Layer-by-layer deposition of EGCG results in direct contact of nanotubes with metal electrodes, thereby reducing the contact resistance.

The proposed mechanism for the conductance response to H_2O_2 is derived from the antioxidant properties of EGCG, which has been the subject of much debate.[40−42] Catechins are oxidized by radicals and thus lose electrons, which segues into the response for SWNT/EGCG devices. Presumably, interactions between EGCG and SWNTs are such that some electron density is transferred between the species. As EGCG is oxidized and loses electrons, it may be that this causes subsequent withdrawal of electron density from the nanotube network, resulting in an increase in the majority charge carrier, holes, and increasing conductance.

To further investigate the mechanism of the conductance response of SWNT/EGCG composite to H_2O_2, we designed another experiment in which an Fe_2O_3 nanoparticle solution was drop-casted on the electrodes modified with SWNTs and EGCG using layer-by-layer

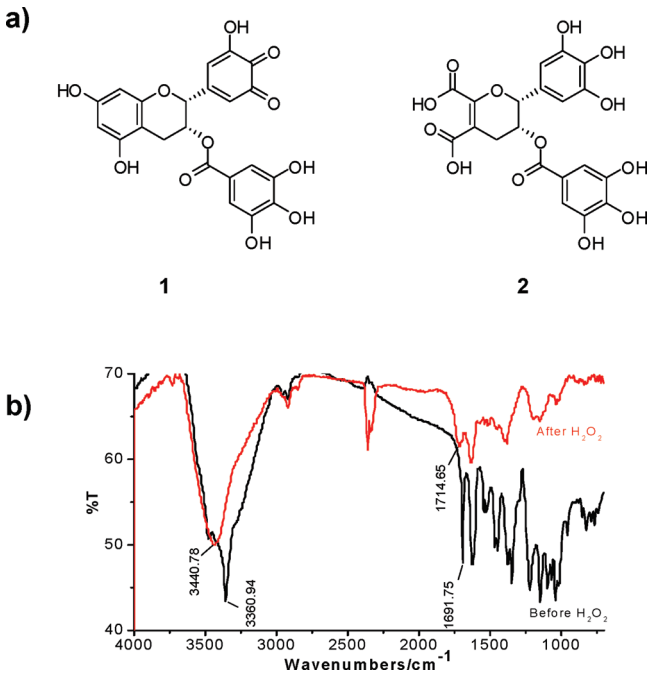

Figure 4. (a) Chemical structures of possible oxidation products of EGCG with H_2O_2 (refs 23 and 40). (b) FTIR spectrum of SWNT/EGCG composite before (black) and after exposure to 10^{-2} M H_2O_2 (red).

setup (Figure 3d,e). While the SWNT/(Fe_2O_3 NP) system showed insignificant improvement for H_2O_2 detection over bare SWNTs and worse performance compared to SWNT/EGCG, a combination of EGCG and Fe_2O_3 nanoparticles has positive synergy for H_2O_2 detection with SWNTs. As can be seen from a calibration plot for SWNT/EGCG and SWNT/EGCG/(Fe_2O_3 NP) devices (Figure 3f), the H_2O_2 responses can be increased to more than 100%, due to the presence of Fe_2O_3 nanoparticles. A similar effect was observed when the SWNT/EGCG composite was mixed with Fe_2O_3 nanoparticles and drop-casted on the device chip. Compared to Figure 3a, a significant increase in H_2O_2 signal was observed (Figure S8). The observed increase in H_2O_2 signal can be explained by the additional ●OH generation *via* Fenton's catalysis mechanism shown in Figure 3g. The Fe^{3+} ions from the Fe_2O_3 nanoparticles first coordinate with EGCG phenol group, followed by subsequent semiquinone formation, and reduction of Fe^{3+} to form quinone species and Fe^{2+}.[43,44] The Fe^{2+} ions formed in this process will then react with H_2O_2 to form reactive oxygen species ●OH, which in turn will oxidize EGCG. The higher degree of EGCG oxidation leads to the observed increased relative conductance response of the SWNT/EGCG composite. This further suggests that the relative conductance response of SWNT/EGCG composites to H_2O_2 arises from the antioxidant property of EGCG and the electron transfer between SWNTs and EGCG.

To confirm that EGCG is actually oxidized upon H_2O_2 exposure, we analyzed FTIR spectra of the composite before and after exposure to 10^{-2} M H_2O_2. Figure 4a shows the possible oxidation products of EGCG with H_2O_2.[23,40] As can be seen in Figure 4b, the peak changes (from 1601 to 1714 cm^{-1} and from 3360 to 3440 cm^{-1}) indicate the formations of quinone groups and a carboxyl group, characteristic of EGCG oxidation products (**1** and **2**). We hypothesize that EGCG oxidation and the subsequent electron transfer lead to the SWNT/EGCG composite response to H_2O_2.

To further understand the sensing mechanism and show application of green tea in chemical sensing, we studied the effect of H_2O_2 concentrations on SWNT/green tea composite conductance in a liquid gate FET configuration. It has been demonstrated in earlier reports that an electrolyte-gated FET configuration can be effectively used for understanding the interaction of various molecules (charged ions or biomolecules) with SWNTs.[45−47] Figure 5a shows the I_d *versus* V_{lg} for a SWNT/green tea composite device measured at different concentrations of H_2O_2. A gradual shift in the threshold voltage for each curve was observed with the increasing concentrations of H_2O_2 from 10^{-4} to 10^{-2}

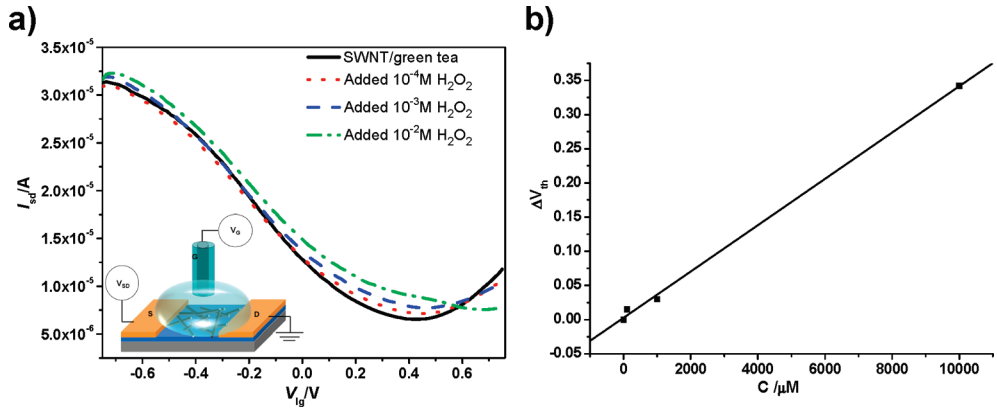

Figure 5. (a) Current *versus* liquid gate potential curves of SWNT/green tea composite device acquired before (black solid) and after adding 10^{-4} M (red dot), 10^{-3} M (blue dash), and 10^{-2} M (green dot dash) H_2O_2. Inset shows the schematic illustration of the liquid gate FET testing device setup. (b) Threshold voltage shift *versus* H_2O_2 concentration plot.

M (Figure 5b). This shift toward positive gate voltages indicates a p-doping of the FET device, which can be attributed to electron withdrawal from the channel by the H_2O_2 molecules. These results strongly correlate with the SWNT/EGCG data shown in Figure 3a, which show the increase in relative conductance with increasing concentrations of H_2O_2.

CONCLUSION

In conclusion, we studied SWNT/green tea and SWNT/EGCG composites using various characterization methods and, most importantly, present here the chemical sensitivity of the composites to ROS. Because of EGCG's antioxidant properties and hydrophilic nature, this composite exhibits sensitivity to hydrogen peroxide in aqueous solution. We propose that these responses are the result of the oxidation of EGCG and electron transfer between EGCG and SWNTs. The H_2O_2 response was further improved by changes in the device architecture and the use of Fe_2O_3 nanoparticles, which promote ROS formation through Fenton's catalysis. Such solid-state electrical measurements indicate that SWNTs functionalized with common or garden green tea have great potential for electronic detection of ROS.

METHODS

Materials. HiPco single-walled carbon nanotubes (SWNTs) were purchased from Carbon Nanotechnologies, Inc. (Grade/Lot# P2/P0329). Epigallocatechin gallate hydrate (EGCG) was obtained from TCI America, and green tea was purchased from Amore Pacific. *N*,*N*-Dimethylformamide (DMF) and hydrogen peroxide (30%) were purchased from EMD chemical and J. T. Baker, respectively. Fe_2O_3 nanoparticles were purchased as nanopowder from Sigma (544884, <50 nm). All reagents were used as received without further purification.

Preparation of SWNT and Green Tea or EGCG Composites. The fabrication of the composites was carried out by sonicating approximately 1 mg of SWNTs in 20 mL of 0.3 mg/mL green tea (or 4×10^{-4} M EGCG) at room temperature (Sonicator: Branson 5510) for 1 h. The solution was then centrifuged (Fisher Scientific centrific model 228) at 3400 rpm for 15 min. The supernatant was then filtered and washed with deionized water subsequently to remove any unbound green tea (EGCG). The resulting material was then dispersed in water to obtain SWNT/green tea (SWNT/EGCG) suspension (resulting concentration 0.05 mg/mL).

Thin films on quartz slides for spectroscopic analysis were made by spray coating a heated quartz slide (140 °C) with the above SWNT/green tea (SWNT/EGCG) suspension. Thin film of bare SWNTs were prepared by spray coating SWNT suspension in DMF at 180 °C.

Thin Film Characterization. Spectroscopic measurements were made using a UV−vis−NIR spectrophotometer (Lambda 900, Perkin-Elmer Instruments). FTIR was performed on a Nicolet Avatar 360 FTIR spectrometer. SWNT/EGCG composite (solid) was ground with KBr finely, and the powder mixture was then crushed in a mechanical die press to form a translucent pellet through which the beam of the spectrometer can pass. SWNT/EGCG composite after exposure to H_2O_2 in solution was filtered and dried. A pellet of this material was made in the same way as mentioned above. FTIR of EGCG was taken by drop-casting and drying a solution of EGCG in methanol on a NaCl salt window.

Scanning electron microscopy (SEM) was performed on a Philips XL30 FEG microscope at an accelerating voltage of 10 keV to characterize the morphology of deposited thin films. Transmission electron microscopy (TEM) images were obtained with a Philips/FEI Morgagni microscope. The electron-beam accelerating voltage of the TEM was held constant at 80 keV for all imaging. All samples were suspended in water, drop-casted onto a lacey-carbon TEM grid (Pacific Grid-Tech), and allowed to dry in ambient conditions. Atomic force microscopy (AFM) characterization was carried out on a Multimode scanning-probe microscope (Veeco). Samples were prepared by spin-coating SWNT/EGCG composite (suspended in water) onto a freshly cleaved sheet of mica surface. After 45 min of drying in ambient conditions, the images were taken. Tapping-mode experiments using supersharp tips (AppNano ACL-SS) (2 nm) allowed for the intricate characterization of all samples. Raman measurements of the thin films were performed on a Renishaw inVia Raman microscope (excitation wavelength 633 nm).

Metal interdigitated devices (Au/Ti, 100 nm/30 nm) with interelectrode spacing of 10 μm were patterned on a Si/SiO_2 substrate using conventional photolithography. One chip (2 mm × 2 mm) containing four identical devices was then set into a 40-pin ceramic dual in-line package (CERDIP) and wire-bonded using Au wire. Devices were subsequently isolated from the rest of the package by epoxying the inner cavity. Fabrication of bare SWNTs' conductance measurement was made by sonicating approximately 1 mg of SWNTs in 20 mL of DMF and drop-casting 40 μL of the dispersion directly on the Si chip in the package device mentioned above. The fabrication of SWNT/EGCG composite devices was carried out by drop-casting 40 μL of a SWNT/EGCG suspension on a chip and allowing it to dry in ambient conditions. For the layer-by-layer SWNT/EGCG device architecture, SWNTs were first deposited onto the electrodes by dielectrophoresis (DEP) method using a SWNT suspension in DMF (Agilent 33250A 80 MHz Function/Arbitrary Waveform Generator, 10 MHz, 8.00 Vpp). After washing with DMF and drying at 180 °C, the devices were incubated with 4.4×10^{-4} M EGCG solution. For SWNTs/EGCG/Fe_2O_3 nanoparticle devices, a SWNT/EGCG device was first prepared and Fe_2O_3 nanoparticle suspension in water was then drop-casted on the electrodes and allowed to dry.

Conductance measurements on composite devices were carried out on a custom test-board using Zephyr software.[31] Using a Keithley 2602 dual-source meter and Keithley 708A switching mainframe, we were able to monitor all devices on a single chip at a given time. Device switching was performed at 500 ms, displaying near-real-time responses for each device.

To investigate the sensing mechanism of H_2O_2 and show application of green tea in chemical sensing, we studied the response of the SWNT/green tea composite in a three-electrode electrolyte-gated field-effect transistor (FET) configuration. In this setup, a home-built fluid chamber was mounted on the CERDIP package to hold a small volume (100 μL) of electrolyte. The conductance of the SWNT transistor device was tuned using double-distilled water as electrolyte, as depicted in Figure 5a. A Ag/AgCl reference electrode connected to a voltage source (Keithley 4200) was used a gate electrode. A liquid gate potential was applied to the reference electrode with respect to grounded drain electrode, while maintaining a constant bias voltage (10 mV) between the source and drain voltage. To obtain a negligible leakage current (10 nA), the gate potential was scanned from −750 to 750 mV.

Acknowledgment. The project described was supported by NIEHS R01ES019304. Y.D.L. acknowledges support of the Korea Research Foundation Grant (KRF-2007-357-D00051) funded by the Korean Government (MOEHRD). We thank the Department of Materials Science and Engineering at the University of Pittsburgh for access to the SEM and TEM instrumentation.

Supporting Information Available: Thermogravimetric analysis (TGA), Raman spectroscopy, atomic force microscopy (AFM), and transmission electron microscopy (TEM) characterizations of the composite, AFM images of SWNT/EGCG thin film thickness before and after water exposure, conductance of SWNT/EGCG thin film immersed in water, responses of bare SWNTs to H_2O_2 vapors

and relative humidity (RH), optical images of SWNT/EGCG composite before and after exposing to high humidity, relative conductance *versus* time response to H_2O_2 of SWNT/EGCG/(Fe_2O_3 nanoparticle) composite, and calculation of the SWNT/EGCG and bare SWNT thin films conductivities available. This material is available free of charge *via* the Internet at http://pubs.acs.org.

REFERENCES AND NOTES

1. Baughman, R. H.; Zakhidov, A. A.; de Heer, W. A. Carbon Nanotubes—The Route toward Applications. *Science* **2002**, *297*, 787–792.
2. Avouris, P. Molecular Electronics with Carbon Nanotubes. *Acc. Chem. Res.* **2002**, *35*, 1026–1034.
3. Kauffman, D. R.; Star, A. Carbon Nanotube Gas and Vapor Sensors. *Angew. Chem., Int. Ed.* **2008**, *47*, 6550−6570; *Angew. Chem.* **2008**, *120*, 6652−6673.
4. Zhao, Q.; Gan, Z.; Zhuang, Q. Electrochemical Sensors Based on Carbon Nanotubes. *Electroanalysis* **2002**, *14*, 1609–1613.
5. Smart, S. K.; Cassady, A. I.; Lu, G. Q.; Martin, D. J. The Biocompatibility of Carbon Nanotubes. *Carbon* **2006**, *44*, 1034–1047.
6. Balasubramanian, K.; Burghard, M. Biosensors Based on Carbon Nanotubes. *Anal. Bioanal. Chem.* **2006**, *385*, 452–468.
7. Bianco, A.; Kostarelos, K.; Prato, M. Applications of Carbon Nanotubes in Drug Delivery. *Curr. Opin. Chem. Biol.* **2005**, *9*, 674–679.
8. Allen, B. L.; Kichambare, P. D.; Star, A. Carbon Nanotube Field-Effect-Transistor-Based Biosensors. *Adv. Mater.* **2007**, *19*, 1439–1451.
9. Moore, V. C.; Strano, M. S.; Haroz, E. H.; Hauge, R. H.; Smalley, R. E.; Schmidt, J.; Talmon, Y. Individually Suspended Single-Walled Carbon Nanotubes in Various Surfactants. *Nano Lett.* **2003**, *3*, 1379–1382.
10. O'Connell, M. J.; Boul, P.; Ericson, L. M.; Huffman, C.; Wang, Y.; Haroz, E.; Kuper, C.; Tour, J.; Ausman, K. D.; Smalley, R. E. Reversible Water-Solubilization of Single-Walled Carbon Nanotubes by Polymer Wrapping. *Chem. Phys. Lett.* **2001**, *342*, 265–271.
11. Star, A.; Stoddart, J. F.; Steuerman, D.; Diehl, M.; Boukai, A.; Wong, E. W.; Yang, X.; Chung, S. W.; Choi, H.; Heath, J. R. Preparation and Properties of Polymer-Wrapped Single-Walled Carbon Nanotubes. *Angew. Chem., Int. Ed.* **2001**, *40*, 1721−1725.
12. Zheng, M.; Jagota, A.; Semke, E. D.; Diner, B. A.; Mclean, R. S.; Lustig, S. R.; Richardson, R. E.; Tassi, N. G. DNA-Assisted Dispersion and Separation of Carbon Nanotubes. *Nat. Mater.* **2003**, *2*, 338–342.
13. Xie, H.; Ortiz-Acevedo, A.; Zorbas, V.; Baughman, R. H.; Draper, R. K.; Musselman, I. H.; Dalton, A. B.; Dieckmann, G. R. Peptide Cross-Linking Modulated Stability and Assembly of Peptide-Wrapped Single-Walled Carbon Nanotubes. *J. Mater. Chem.* **2005**, *15*, 1734–1741.
14. Karajanagi, S. S.; Yang, H.; Asuri, P.; Sellitto, E.; Dordick, J. S.; Kane, R. S. Protein-Assisted Solubilization of Single-Walled Carbon Nanotubes. *Langmuir* **2006**, *22*, 1392–1395.
15. Star, A.; Steuerman, D. W.; Heath, J. R.; Stoddart, J. F. Starched Carbon Nanotubes. *Angew. Chem., Int. Ed.* **2002**, *41*, 2508−2512.
16. Nakamura, G.; Narimatsu, K.; Niidome, Y.; Nakashima, N. Green Tea Solution Individually Solubilizes Single-Walled Carbon Nanotubes. *Chem. Lett.* **2007**, *9*, 1140–1141.
17. Khan, S. G.; Katiyar, S. K.; Agarwal, R.; Mukhtar, H. Enhancement of Antioxidant and Phase II Enzymes by Oral Feeding of Green Tea Polyphenols in Drinking Water to SKH-1 Hairless Mice: Possible Role in Cancer Chemoprevention. *Cancer Res.* **1992**, *52*, 4050–4052.
18. Chang, C. J.; Chiua, K.-L.; Chen, Y. -L.; Chang, C.-Y. Separation of Catechins from Green Tea Using Carbon Dioxide Extraction. *Food Chem.* **2000**, *68*, 109–113.
19. Mochizuki, M.; Yamazaki, S.-I.; Kano, K.; Ikeda, T. Kinetic Analysis and Mechanistic Aspects of Autoxidation of Catehins. *Biochim. Biophys. Acta* **2002**, *1569*, 35–44.
20. Valcic, S.; Muders, A.; Jacobsen, N. E.; Liebler, D. C.; Timmermann, B. N. Antioxidant Chemistry of Green Tea Catechins. Identification of Products of the Reaction of (−)-Epigallocatechin Gallate with Peroxyl Radicals. *Chem. Res. Toxicol.* **1999**, *12*, 382–386.
21. Lee, S.-R.; Im, K.-J.; Suh, S.-I.; Jung, J.-G. Protective Effect of Green Tea Polyphenol (−)-Epigallocatechin Gallate and Other Antioxidants on Lipid Peroxidation in Gerbil Brain Homogenates. *Phytother. Res.* **2003**, *17*, 206–209.
22. Sadzuka, Y.; Sugiyama, T.; Sonobe, T. Efficacies of Tea Components on Doxorubicin Induced Antitumor Activity and Reversal of Multidrug Resistance. *Toxicol. Lett.* **2000**, *114*, 155–162.
23. Zhu, N.; Huang, T.-C.; Yu, Y.; LaVoie, E. J.; Yang, C. S.; Ho, C.-T. Identification of Oxidation Products of (−)-Epigallocatechin Gallate and (−)-Epigallocatechin with H_2O_2. *J. Agric. Food Chem.* **2000**, *48*, 979–981.
24. Annabi, B.; Bouzeghrane, M.; Moumdjian, R.; Moghrabi, A.; Beliveau, R. Probing the Infiltrating Character of Brain Tumors: Inhibition of Rhoa/ROK-Mediated CD44 Cell Surface Shedding from Glioma Cells by the Green Tea Catechin EGCG. *J. Neurochem.* **2005**, *94*, 906–916.
25. Morré, D. M.; Morré, D. J. Anticancer Activity of Grape and Grape Skin Extracts Alone and Combined with Green Tea Infusions. *Cancer Lett.* **2006**, *238*, 202–209.
26. Tachibana, H.; Koga, K.; Fujimura, Y.; Yamada, K. A Receptor for Green Tea Polyphenol EGCG. *Nat. Struct. Mol. Biol.* **2004**, *11*, 380–381.
27. Weisburger, J. H. In *Handbook of Anitoxidants*; Cardenas, E., Packer, L., Eds.; Marcel Dekker Inc.: New York, 1996; pp 469−486.
28. Sies, H. Oxidative Stress: Oxidants and Antioxidants. *Exp. Physiol.* **1997**, *82*, 291–295.
29. Fenton, H. J. H. Oxidation of Tartaric Acid in Presence of Iron. *J. Chem. Soc.* **1894**, *65*, 899–910.
30. Landi, B. J.; Evans, C. M.; Worman, J. J.; Castro, S. L.; Bailey, S. G.; Raffaelle, R. P. Noncovalent Attachment of CdSe Quantum Dots to Single Wall Carbon Nanotubes. *Mater. Lett.* **2006**, *60*, 3502–3506.
31. Zephyr Software Open Source: http://zephyr.synopsia.net/.
32. Manatt, S. L.; Manatt, M. R. R. On the Analyses of Mixture Vapor Pressure Data: The Hydrogen Peroxide/Water System and Its Excess Thermodynamic Functions. *Chem.—Eur. J.* **2004**, *10*, 6540–6557.
33. O'Brien, F. E. M. The Control of Humidity by Saturated Salt Solutions. *J. Sci. Instrum.* **1948**, *25*, 73–76.
34. Greenspan, L. Humidity Fixed Points of Binary Saturated Aqueous Solutions. *J. Res. Natl. Bur. Stand.* **1977**, *81*, 89–96.
35. Wang, F.; Gu, H.; Swager, T. M. Carbon Nanotube/Polythiophene Chemiresistive Sensors for Chemical Warfare Agents. *J. Am. Chem. Soc.* **2008**, *130*, 5392–5393.
36. Star, A.; Han, T.-R.; Joshi, V.; Stetter, J. R. Sensing with Nafion Coated Carbon Nanotube Field-Effect Transistors. *Electroanalysis* **2004**, *16*, 108–112.
37. Kim, W.; Javey, A.; Vermesh, O.; Wang, Q.; Li, Y.; Dai, H. Hysteresis Caused by Water Molecules in Carbon Nanotube Field-Effect Transistors. *Nano Lett.* **2003**, *3*, 193–198.
38. Zhang, Z. B.; Liu, X. J.; Campbell, E. E.; Zhang, S. L. Alternating Current Dielectrophoresis of Carbon Nanotubes. *J. Appl. Phys.* **2005**, *98*, 056103.
39. Lim, J.-H.; Phiboolsirichit, N.; Mubeen, S.; Rheem, Y.; Deshusses, M. A.; Mulchandani, A.; Myung, N. V. Electrical and Sensing Properties of Single-Walled Carbon Nanotubes Network: Effect of Alignment and Selective Breakdown. *Electroanalysis* **2010**, *22*, 99–105.
40. Kondo, K.; Kurihara, M.; Miyata, N.; Suzuki, T.; Toyoda, M. Mechanistic Studies of Catechins as Antioxidants against Radical Oxidation. *Arch. Biochem. Biophys.* **1999**, *362*, 79–86.
41. Yoshioka, H.; Sugiura, K.; Kawahara, R.; Fujita, T.; Makino, M.; Kamiya, M.; Tsuyumu, S. Formation of Radicals and Chemiluminescence during the Autoxidation of Tea Catechins. *Agric. Biol. Chem.* **1991**, *55*, 2717–2723.

42. Severino, J. F.; Goodman, B. A.; Kay, C. W. M.; Stolze, K.; Tunega, D.; Reichenauer, T. G.; Pirker, K. F. Free Radicals Generated during Oxidation of Green Tea Polyphenols: Electron Paramagnetic Resonance Spectroscopy Combined with Density Functional Theory Calculations. *Free Radical Biol. Med.* **2009**, *46*, 1076–1088.
43. Perron, N. R.; Brumaghim, J. L. A Review of the Antioxidant Mechanisms of Polyphenol Compounds Related to Iron Binding. *Cell Biochem. Biophys.* **2009**, *53*, 75–100.
44. Ryan, P.; Hynes, M. J. The Kinetics and Mechanisms of the Complex Formation and Antioxidant Behaviour of the Polyphenols EGCG and ECG with Iron(III). *J. Inorg. Biochem.* **2007**, *101*, 585–593.
45. Rosenblatt, S.; Yaish, Y.; Park, J.; Gore, J.; Sazonova, V.; McEuen, P. L. High Performance Electrolyte Gated Carbon Nanotube Transistors. *Nano Lett.* **2002**, *2*, 869–872.
46. Krüger, M.; Buitelaar, M. R.; Nussbaumer, T.; Schönenberger, C.; Forró, L. Electrochemical Carbon Nanotube Field-Effect Transistor. *Appl. Phys. Lett.* **2001**, *78*, 1291–1293.
47. Heller, I.; Janssens, A. M.; Männik, J.; Minot, E. D.; Lemay, S. G.; Dekker, C. Identifying the Mechanism of Biosensing with Carbon Nanotube Transistors. *Nano Lett.* **2008**, *8*, 591–595.